

EFFECTIVE AUDIO CLASSIFICATION NETWORK BASED ON PAIRED INVERSE PYRAMID STRUCTURE AND DENSE MLP BLOCK

Yunhao Chen^{*†1}, Yunjie Zhu^{*2}, Zihui Yan^{*1},

Lifang Chen^{†1}

Jiangnan University¹
School of Artificial Intelligence and Computer Science
Wuxi, 214000, China

University of Leeds²
School of Computing
Leeds, LS2 9JT, United Kingdom

ABSTRACT

Recently, massive architectures based on Convolutional Neural Network (CNN) and self-attention mechanisms have become necessary for audio classification. While these techniques are state-of-the-art, these works' effectiveness can only be guaranteed with huge computational costs and parameters, large amounts of data augmentation, transfer from large datasets and some other tricks. By utilizing the lightweight nature of audio, we propose an efficient network structure called Paired Inverse Pyramid Structure (PIP) and a network called Paired Inverse Pyramid Structure MLP Network (PIPMN). The PIPMN reaches 96% of Environmental Sound Classification (ESC) accuracy on the UrbanSound8K dataset and 93.2% of Music Genre Classification (MGC) on the GTAZN dataset, with only 1 million parameters. Both of the results are achieved without data augmentation or model transfer. Public code is available at:

<https://github.com/JNAIC/PIPMN>.

Index Terms— Environmental sound classification, music genre classification, multi-stage structure, skip connection, multi-layer perceptron (MLP)

1. INTRODUCTION

The audio classification aims to classify sounds into several human-defined categories, such as ESC [1] or MGC tasks[2]. In recent years, more and more researchers have been developing audio classification systems which can accurately classify various types of sounds. The audio classification tasks like the ESC, for example, can be applied to the hearing aid [3], urban planning [4], biology [5], and the MGC can be applied to music recommend systems or emotional tests [6,7].

The deep learning technique has demonstrated state-of-the-art accuracy in audio classification, especially the convolutional neural network (CNN) and self-attention mechanism. For the CNN-based or attention-based models, the audio is usually extracted as the 2D spectrogram and processed as images [8-10]. More recently, transfer learning [11] from large

datasets knowledge distillation [12] and cross-modal cooperative learning [13] have been utilized to help models become robust and improve their accuracy.

Nevertheless, the audio is different from the image. From the perspective of dimension, the audio spectrum is 2D data, and the image is 3D data (with channels). Therefore, if we only regard the audio spectrum as an Image, the frequency or cepstral coefficients domain (called depth domain thereafter) and temporal domain will be processed as the spatial domain together like images. Moreover, they must add a new dimension for the input data as the channel to fit the input data in the Image model. Consequently, the computational cost of the model will increase and overfit easily. Previous works [14-16] in this area demonstrate improvement in the ESC task. However, despite their success, they still have a limitation: their networks primarily focus on the spatial information of the time and frequency domain and fail to extract depth domain information adequately. This limitation results in lower accuracy.

Moreover, the simple and computational-saving module MLP has already demonstrated its competitiveness in the image classification task [17] on the ImageNet [18], during which the MLP architecture achieves similar results compared with CNN and transformer. Based on the results, we believe that the MLP can extract information from complex situations. Consequently, we construct our network based on MLP. Nonetheless, the current multi-stage structure [19] for CNN is unsuitable for MLP-based networks. Because based on our experiments, the MLP network overfits more easily under the same multi-stage structure. To solve this problem, we propose a long-range skip connection with layer scale [20] on the bottleneck to reduce overfitting.

In this paper, we devised a new way to extract the information in the depth domain and time domain for audio classification with as few parameters as possible. We have three motivations. The first one is to process the audio using its lightweight nature instead of regarding it as an image. The second is replacing CNN and transformer with MLP to save computational cost and parameters. Based on these two motivations, we propose the Dense MLP(DM) block for audio classification. The third one is to reduce the network's overfitting. Based on this motivation, we propose the Paired Inverse Pyramid Structure (PIP).

[†] Corresponding authors

^{*} These authors contribute equally to this work and should be considered co-first authors.

To summarize, the main contributions of this paper are as follows:

- 1) We propose a Dense MLP block to extract audio’s spatial and temporal domain information more effectively.
- 2) We propose a Paired Inverse Pyramid Structure to reduce overfitting for multi-stage MLP networks in audio classification.
- 3) The entire PIPMN achieves outstanding accuracy on both the UrbanSound8K dataset for the ESC task and the GTAZN dataset for the MGC task without data augmentation and model transfer.

2. METHODS

2.1. Paired Inverse Pyramid Structure

The whole structure is depicted in Figure 1. The long-range skip connection with layer scale on the bottleneck can reduce overfitting. The reason is that, as the original multi-stage structure goes deeper, the function represented by the network becomes more complex due to more parameters. Consequently, the network is more likely to overfit. However, with the training dynamics [20] offered by layer scale, the network can fit from a less complex function represented by the skip connection. As a result, the structure is less likely to overfit.

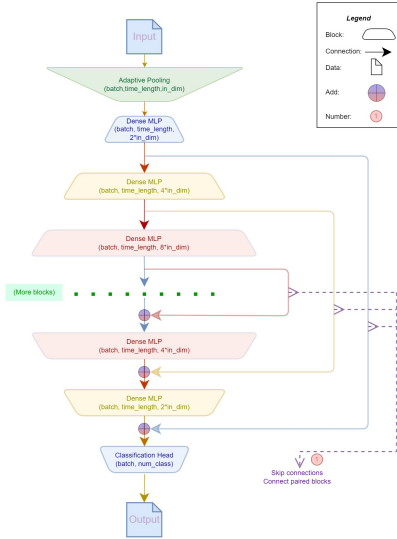


Fig. 1. Paired Inverse Pyramid Structure.

Moreover, experiments on deep networks with stochastic depth [21] show that the learning of a layer relies on the information retrieved from the last layer and on the information retrieved from the layer that is not adjacent to it. Consequently, the information passed through a long-range skip connection can ensure the information extracted by a layer goes to another layer that needs it without going through multiple intermediate layers and being lost.

2.2. Positional Modelling for Time Domain and Depth Domain

The spectrogram fed into the positional modelling can be represented as $\chi \in \mathbb{R}^{B \times D \times L}$ where B is the batch size, L is the temporal domain, and D is the Depth domain. And the positional modelling for the depth domain on the time domain can be described as follows:

$$\varphi(\chi) = \chi * \gamma_3^1 \quad (1)$$

where $\varphi(\chi)$ is the positional modelling, the γ_3^1 is convolution layer with a kernel size of 3 and stride of 1. To fit the positional modelling to the network, we used the 1-padding on both ends of the temporal domain in the layer. To reduce parameters, the group of input equals to D.

2.3. Feed-Forward Structure for Temporal MLP

The structure is illustrated in Figure 2. The feed-forward structure includes one skip connection [22], one MLP block and a positional modelling block. The MLP block includes one LayerNorm [23] layer, two Linear layers and a GELU [24] activation function. Like the transformer structure[25], the MLP block expands the time domain length and then shrinks to the original length to better exploit the information in the time domain. A hyperparameter called α controls the expansion ratio. The MLP block can be described using the following equation:

$$\phi(\chi) = W_{L \times \alpha L}^T (GELU(W_{\alpha L \times L}^T (\eta(\chi)) + b_1)) + b_2 \quad (2)$$

where $\chi \in \mathbb{R}^{B \times D \times L}$, $\eta(\chi)$ is the layer normalization for χ , $W_{a \times b}$ is the learnable parameters vector of size $a \times b$, b_1, b_2 is the corresponding bias, and GELU is the activation function. The whole feed-forward structure can be described as follows:

$$\gamma(\chi) = W_{3\alpha L \times L}^T ([\varphi(\chi), \chi, \phi(\chi)]) \quad (3)$$

where $\chi \in \mathbb{R}^{B \times D \times L}$, $\phi(\chi)$ is the operation in the MLP, $[\dots]$ is the concatenation operation between tensors, and $W_{3\alpha L \times L}$ transforms the size of the concatenation tensor into the original one. This feed-forward structure aims to extract the information related to the temporal domain and the relations between the temporal and depth domain.

2.4. Depth Domain Block

Due to the complicated structure of PIP, the depth domain block of each dense MLP block is relatively simple to reduce overfitting, which will not compromise its overall accuracy and will be less likely to overfit. The structure is depicted in Figure 3 and can be described as follows:

$$\delta(\chi) = GELU(W_{D_{in} \times D_{out}}^T \eta(\chi)) + \omega_{D_{in} \times D_{out}}^T (\chi) \quad (4)$$

where $w_{D_{in} \times D_{out}}$ is the learnable parameters vector of size $D_{in} \times D_{out}$ and $\chi \in \mathbb{R}^{B \times L \times D}$ (its size permutation is different from the tensor χ mentioned above). What needs to be

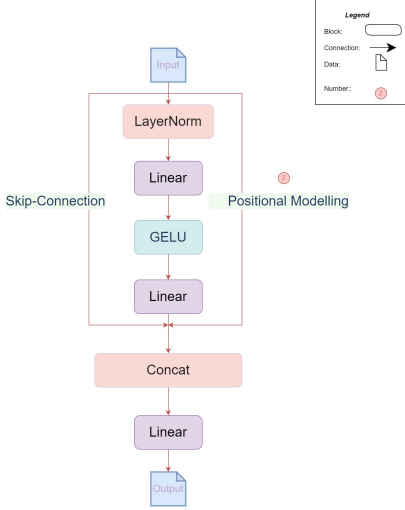


Fig. 2. Feed-Forward Structure for Temporal MLP.

emphasized is the special skip connection for this layer. Because the tensor size of this layer’s output differs from the input’s size, we need to add a simple Linear layer for the input to fit the skip connection into the structure. And the skip connection works because it gives a simple way for transforming and mapping the original data to the processed data. Without this skip connection, the information forwarded by multi-layers will be lost due to multiple transformations. Also, compared with the inherited complex structure of a deep neural network, a simple Linear layer is simple enough to become the skip connection in aspects of transformation. Consequently, a Linear layer can work as the skip connection which was implemented with identity shortcut in the ResNet. Therefore, the module functioning as the skip connection is named as the Linear Skip Connection.

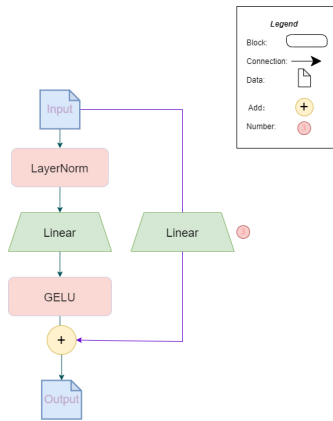


Fig. 3. The Structure of Depth Domain Block.

2.5. Dense MLP

The whole structure is depicted in Figure 4. And the processing procedure for the structure can be described as fol-

lows:

$$\theta(\chi) = \epsilon_2 \delta(\epsilon_1 \lambda(\gamma(\lambda(\chi)))) + \chi \quad (5)$$

where $\lambda(\chi)$ is the operation of permutation between the depth domain and temporal domain, the operation transforms the $\chi \in \mathbb{R}^{B \times L \times D}$ into $\chi \in \mathbb{R}^{B \times D \times L}$ or transforms the $\chi \in \mathbb{R}^{B \times D \times L}$ into $\chi \in \mathbb{R}^{B \times L \times D}$. ϵ_1, ϵ_2 means learnable scalars as the layer scale value[20], which can reduce the overfitting according to the experiments.

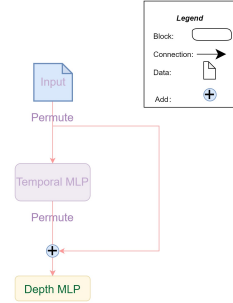


Fig. 4. The Structure of Dense MLP.

3. EXPERIMENTS

3.1. Training setup and Preprocessing for the Datasets

We evaluate our approach on the UrbanSound8K dataset for the ESC and the GTZAN dataset for the MGC. For the input tensor, NGCC [26], MFCC, GFCC [27], LFCC [28] and BFCC [29] features are extracted with the size of (399,20) for each feature (the window length is 0.025s and the hop length is 0.01s). Also, what needs to emphasize is that each sample in the GTZAN dataset has 30s second length. To fit the input size to our model, we cut each sample into 7 segments. Consequently, audio samples in both datasets are 4s in length. Also, the training batch size is 128. As a result, the input size is (128,399,100). We used the AdamW optimizer in the experiments with a learning rate of 0.001, a weight-decay of 0.05 and other parameters are default. The loss we used in the experiments is the Cross-entropy-loss with label-smoothing of 0.1. The training epochs are 3500 for the two datasets. To prove the efficiency of our network, we did not use techniques like data augmentation, model transfer, EMA, pretraining, or others. We used 10-Fold for performance evaluation.

3.2. UrbanSound8K Experiments Results

Table 1 compares our model’s effectiveness with other works on the UrbanSound8K dataset. The table shows that our proposed model achieves state-of-the-art results without data augmentation. Consequently, our model can retrieve helpful information without too much overfitting. Moreover, our model is better than these models, not only in terms of accuracy but also the parameter size.

Table 1: PREVIOUS STATE-OF-THE-ART ESC MODELS VS. THE PROPOSED MODEL IN THIS PAPER ON URBANSOUND8K DATASET

Framework	Classification Accuracy(%)	Parameters	Ref.
EAT-M*#	90	25.5M	[30]
EAT-S*#	88.1	5.3M	[30]
ESResNeXt-fbsp*	89.14	25M	[31]
ERANN-1-4*#	83.5	24.1M	[32]
ESResnet-Att	82.76	32.6M	[33]
ERANN-2-6*#	90.8	54.5M	[32]
Proposed model	96	1.4M	-

*means data augmentation is used # means model pretrained is used.

3.3. GTZAN Experiments Results

To further explain the efficiency of our model, we evaluate our model on the GTZAN dataset for the MGC task.

Table 2: PREVIOUS STATE-OF-THE-ART ESC MODELS VS. THE PROPOSED MODEL IN THIS PAPER ON GTZAN DATASET

Framework	Classification Accuracy(%)	Parameters	Ref.
VGGish*#	92.2	72.1M	[34]
VGGish+CoTrans-b2*#	95	72.6M	[34]
Improved-BBNN	91	0.18M	[35-36]
Proposed model	93.3	1.4M	-

As we can see from Table 2, though our model is not state-of-art or the most lightweight model, our model maintains a balance between the parameters and the accuracy. What is more, these models are specialized for the MGC task. Compared with other models, our model is good at both the ESC and MGC tasks. Consequently, we can confidently conclude that our model has scalability in the audio classification.

3.4. Ablation Study on UrbanSound8K

To further investigate the influence of different parts on the classification results, we conduct an ablation study on the UrbanSound8K dataset. To demonstrate the effects of different data preprocessing, we conduct two experiments on the input data. Firstly, we replace the original data input with 50 MFCCs. Secondly, we replace the input with a 100-Mel-Spectrogram. The experiments on the MFCC and Mel-Spectrogram show that the input change does not influence the outcome significantly. Consequently, the results of our model are not highly dependent on the input.

Moreover, to demonstrate the effectiveness of the PIP structure, we replace the PIP structure in the model with the original multi-stage structure. We have also explored the effectiveness of different modules in the Dense MLP. In the

Table 3: ABLATION STUDY ON URBANSOUND8K DATASET

Framework	Classification Accuracy(%)	Parameters
Without ①	93.5	1.4M
Without ②	95.6	1.4M
Without ③	94.2	1.4M
MFCC	95.5	0.3M
Mel-Spectrogram	92.2	1.4M
Original Multi-Stage	94.2	3.6M
Proposed model	96	1.4M

① is Long Range Skip Connection, ② is Positional Modelling, ③ is Linear Skip Connection. The structures represented by these numbers are already indicated in the figures.

experiment, we removed ①, ②, and ③ in sequence. The results of these experiments are shown in Table 3.

The original multi-stage structure is shown in Figure 5. The transition layer in the original multi-stage structure is not shown in Figure 5. It is easy to work out that the original multi-stage structure has much more parameters than the PIP in theory. In Table III, we have shown the effectiveness of our PIP structure compared with the original multi-stage structure.

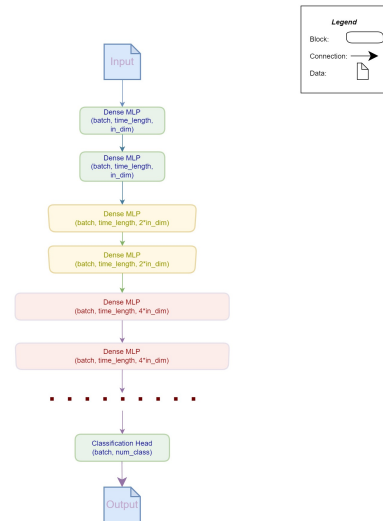


Fig. 5. Original Multi-Stage Structure.

4. CONCLUSION

In this paper, we propose a new network called PIPMN. The proposal of this network is based on the lightweight nature of audio. The results have shown that processing audio as audio instead of the image can achieve state-of-the-art performance with fewer parameters. However, this model only focuses on ESC and MGC. For future work, we will extend our model for more challenging tasks such as sound detection and multi-label classification.

5. REFERENCES

- [1] J. Salamon, C. Jacoby, and J. P. Bello, "A dataset and taxonomy for urban sound research," in Proc. ACM Int. Conf. Multimedia, 2014, pp. 1041–1044.
- [2] Tzanetakis, G., Cook, P.: Musical genre classification of audio signals. *IEEE Trans. Speech Audio Process.* 10(5), 293–302 (2002). Available: <https://doi.org/10.1109/TSA.2002.800560>.
- [3] E. Alexandre, L. Cuadra, M. Rosa, and F. López-Ferreras, "Feature selection for sound classification in hearing aids through restricted search driven by genetic algorithms," *IEEE Trans. Audio, Speech, Lang. Process.*, vol. 15, no. 8, pp. 2249–2256, Nov. 2007, doi: 10.1109/TASL.2007.905139.
- [4] D. Barchiesi, D. D. Giannoulis, D. Stowell, and M. D. Plumbley, "Acoustic scene classification: Classifying environments from the sounds they produce," *IEEE Signal Process. Mag.*, vol. 32, no. 3, pp. 16–34, May 2015, doi: 10.1109/MSP.2014.2326181.
- [5] F. R. González-Hernández, L. P. Sánchez-Fernández, S. Suárez-Guerra, and L. A. Sánchez-Pérez, "Marine mammal sound classification based on a parallel recognition model and octave analysis," *Appl. Acoust.*, vol. 119, pp. 17–28, Apr. 2017, doi: 10.1016/J.APACOUST.2016.11.016.
- [6] George A. Tsihrintzis, Aristomenis S. Lampropoulos, Paraskevi S. Lampropoulou. A Cascade Hybrid Music Recommender System for mobile services based on musical genre classification and personality diagnosis[J]. *Multimedia tools & applications.* 2012, 59(1).
- [7] Michael J. Silverman. Music Based Affect Regulation and Unhealthy Music Use Explain Coping Strategies in Adults with Mental Health Conditions. [J]. *Community Mental Health Journal.* 2020. doi:10.1007/s10597-020-00560-4.
- [8] J. Salamon and J. P. Bello, "Deep convolutional neural networks and data augmentation for environmental sound classification," *IEEE Signal Process. Lett.*, vol. 24, no. 3, pp. 279–283, Mar. 2017.
- [9] J. Huang, H. Lu, P. L. Meyer, H. Cordourier, and J. D. H. Ontiveros, "Acoust. scene classification using deep learning-based ensemble averaging," in Proc. Detection Classification Acoust. Scenes Events Workshop, NY, USA, 2019, pp. 94–98.
- [10] N. RishabhTak, M. DharmeshAgrawal, and H. A. Patil, "Novel phase encoded mel filterbank energies for environmental sound classification," in Proc. Int. Conf. Pattern Recognit. Mach. Intell., 2017, pp. 317–325.
- [11] A. Kumar, M. Khadkevich, and C. Fügen, "Knowledge transfer from weakly labeled audio using convolutional neural network for sound events and scenes," in Proc. IEEE Int. Conf. Acoust., Speech Signal Process., 2018, pp. 326–330.
- [12] A. Kumar and V. Ithapu, "A sequential self teaching approach for improving generalization in sound event recognition," in Proc. 37th Int. Conf. Mach. Learn., 2020, pp. 5447–5457.
- [13] Y. Aytar, C. Vondrick, and A. Torralba, "SoundNet: Learning sound representations from unlabeled video," in Proc. 30th Int. Conf. Neural Inf. Process. Syst., 2016, pp. 892–900.
- [14] L. Zhang, Z. Shi, and J. Han, "Pyramidal temporal pooling with discriminative mapping for audio classification," *IEEE/ACM Trans. Audio, Speech Lang. Process.*, vol. 28, pp. 770–784, 2020.
- [15] L. Zhang, J. Han, and Z. Shi, "Learning temporal relations from semantic neighbors for acoustic scene classification," *IEEE Signal Process. Lett.*, vol. 27, pp. 950–954, 2020.
- [16] L. Zhang, J. Han, and Z. Shi, "ATReSN-Net: Capturing attentive temporal relations in semantic neighborhood for acoustic scene classification," in Proc. Annu. Conf. Int. Speech Commun. Assoc., 2020, pp. 1181–1185.
- [17] I. Tolstikhin et al., "MLP-Mixer: An all-MLP Architecture for Vision", arXiv.org, 2022. [Online]. Available: <https://arxiv.org/abs/2105.01601v3>. [Accessed: 15- Sep- 2022].
- [18] J. Deng, W. Dong, R. Socher, L.-J. Li, K. Li, and L. Fei-Fei. ImageNet: A Large-Scale Hierarchical Image Database. In CVPR09, 2009.
- [19] Z. Liu, H. Mao, C. Wu, C. Feichtenhofer, T. Darrell and S. Xie, "A ConvNet for the 2020s", arXiv.org, 2022. [Online]. Available: <https://arxiv.org/abs/2201.03545v1>. [Accessed: 15- Sep- 2022].
- [20] H. Touvron, M. Cord, A. Sablayrolles, G. Synnaeve and H. Jégou, "Going deeper with Image Transformers", arXiv.org, 2022. [Online]. Available: <https://arxiv.org/abs/2103.17239v2>. [Accessed: 15- Sep- 2022].
- [21] G. Huang, Y. Sun, Z. Liu, D. Sedra and K. Weinberger, "Deep Networks with Stochastic Depth", arXiv.org, 2022. [Online]. Available: <https://arxiv.org/abs/1603.09382>. [Accessed: 15- Sep- 2022].
- [22] K. He, X. Zhang, S. Ren and J. Sun, "Deep Residual Learning for Image Recognition", arXiv.org, 2022. [Online]. Available: <https://arxiv.org/abs/1512.03385v1>. [Accessed: 15- Sep- 2022].
- [23] J. Ba, J. Kiros and G. Hinton, "Layer Normalization", arXiv.org, 2022. [Online]. Available: <https://arxiv.org/abs/1607.06450>. [Accessed: 15- Sep- 2022].
- [24] D. Hendrycks and K. Gimpel, "Gaussian Error Linear Units (GELUs)", arXiv.org, 2022. [Online]. Available: <https://arxiv.org/abs/1606.08415>. [Accessed: 15- Sep- 2022].
- [25] Ashish Vaswani, Noam Shazeer, Niki Parmar, Jakob Uszkoreit, Llion Jones, Aidan N. Gomez, Łukasz Kaiser, and Illia Polosukhin. 2017. Attention is all you need. In Proceedings of the 31st International Conference on Neural Information Processing Systems (NIPS'17). Curran Associates Inc., Red Hook, NY, USA, 6000–6010.
- [26] Zouhir, Youssef & Ouni, Kais. (2016). Feature Extraction Method for Improving Speech Recognition in Noisy Environments. *Journal of Computer Science.* 12, 56-61. 10.3844/jcssp.2016.56.61.
- [27] X. Valero and F. Alias, "Gammatone Cepstral Coefficients: Biologically Inspired Features for Non-Speech Audio Classification," in *IEEE Transactions on Multimedia*, vol. 14, no. 6, pp. 1684–1689, Dec. 2012, doi: 10.1109/TMM.2012.2199972.
- [28] X. Zhou, D. Garcia-Romero, R. Duraiswami, C. Espy-Wilson and S. Shamma, "Linear versus mel frequency cepstral coefficients for speaker recognition," 2011 IEEE Workshop on Automatic Speech Recognition & Understanding, 2011, pp. 559–564, doi: 10.1109/ASRU.2011.6163888.
- [29] Kumar, Chandar, Faizan ur Rehman, Shubash Kumar, Atif Mehmood and Ghulam Shabir. "Analysis of MFCC and BFCC in a speaker identification system." 2018 International Conference on Computing, Mathematics and Engineering Technologies (iCoMET) (2018): 1-5.
- [30] A. Gazneli, G. Zimmerman, T. Ridnik, G. Sharir and A. Noy, "End-to-End Audio Strikes Back: Boosting Augmentations Towards An Efficient Audio Classification Network", arXiv.org, 2022. [Online]. Available: <https://arxiv.org/abs/2204.11479v5>. [Accessed: 15- Sep- 2022].
- [31] Andrey Guzhov, Federico Raue, Jörn Hees, and Andreas Dengel. Esresne(x)-fbasp: Learning robust time-frequency transformation of audio, 2021.
- [32] Sergey Verbitskiy, Vladimir Berikov, and Viacheslav Vyshegorodtsev. Erans: Efficient residual audio neural networks for audio pattern recognition. arXiv preprint arXiv:2106.01621, 2021.
- [33] Andrey Guzhov, Federico Raue, Jörn Hees, and Andreas Dengel. Esresnet: Environmental sound classification based on visual domain models. In 2020 25th International Conference on Pattern Recognition (ICPR), pages 4933–4940. IEEE, 2021.
- [34] L. Hedegaard, A. Bakhtiarnia and A. Iosifidis, "Continual Transformers: Redundancy-Free Attention for Online Inference", arXiv.org, 2022. [Online]. Available: <https://arxiv.org/abs/2201.06268>. [Accessed: 15- Sep- 2022].
- [35] C. Liu, L. Feng, G. Liu, H. Wang and S. Liu, "Bottom-up Broadcast Neural Network For Music Genre Classification", arXiv.org, 2022. [Online]. Available: <https://arxiv.org/abs/1901.08928>. [Accessed: 15- Sep- 2022].
- [36] A. Heakl, A. Abdelgawad and V. Parque, "A Study on Broadcast Networks for Music Genre Classification", arXiv.org, 2022. [Online]. Available: <https://arxiv.org/abs/2208.12086>. [Accessed: 15- Sep- 2022].